Cell, Vol. 111, 251–263, October 18, 2002, Copyright ©2002 by Cell Press

# β-Catenin and TCF Mediate Cell Positioning in the Intestinal Epithelium by Controlling the Expression of EphB/EphrinB

**Eduard Batlle,[1,6] Jeffrey T. Henderson,[2] Harry Beghtel,[1,6] Maaike M.W. van den Born,[1,6] Elena Sancho,[1,6] Gerwin Huls,[1,6] Jan Meeldijk,[1,6] Jennifer Robertson,[3] Marc van de Wetering,[1,6] Tony Pawson,[3,4] and Hans Clevers[1,5,6]**

[1]Department of Immunology and Center for Biomedical Genetics
University Medical Center
Heidelberglaan 100
3584 CX Utrecht
The Netherlands

[2]Department of Pharmaceutical Sciences
Leslie Dan Faculty of Pharmacy
University of Toronto
19 Russell Street
Toronto, Ontario
M5S 262
Canada

[3]Program in Molecular Biology and Cancer
Samuel Lunenfeld Research Institute
Mount Sinai Hospital
600 University Avenue
Toronto, Ontario
M5G 1X5
Canada

[4]Department of Medical Genetics and Microbiology
University of Toronto
Toronto, Ontario
M5S 1A8
Canada

## Summary

**In the small intestine, the progeny of stem cells migrate in precise patterns. Absorptive, enteroendocrine, and goblet cells migrate toward the villus while Paneth cells occupy the bottom of the crypts. We show here that β-catenin and TCF inversely control the expression of the EphB2/EphB3 receptors and their ligand ephrin-B1 in colorectal cancer and along the crypt-villus axis. Disruption of *EphB2* and *EphB3* genes reveals that their gene products restrict cell intermingling and allocate cell populations within the intestinal epithelium. In *EphB2*/*EphB3* null mice, the proliferative and differentiated populations intermingle. In adult *EphB3*$^{-/-}$ mice, Paneth cells do not follow their downward migratory path, but scatter along crypt and villus. We conclude that in the intestinal epithelium β-catenin and TCF couple proliferation and differentiation to the sorting of cell populations through the EphB/ephrin-B system.**

## Introduction

Cell renewal, lineage commitment, and cell differentiation in the mammalian intestinal epithelium occur throughout postnatal life. These processes are intimately coupled to cell migration in a precise, spatially organized manner. At the bottom of the crypts, stem cells give rise to a transient population of undifferentiated cells that vigorously proliferate as they migrate toward the lumen of the intestine. These precursors commit to different cell lineages during their migration and undergo cell cycle arrest and differentiation upon reaching the top of the crypts. This basic pattern of cell behavior is conserved in the small intestine, with one significant difference, namely that the precursors follow a bidirectional migratory path. Goblet, enteroendocrine, and absorptive cells migrate toward the lumen of the gut, but Paneth cells migrate toward the bottom of the crypt (Stappenbeck et al., 1998; Potten and Loeffler, 1990). Little is known about the mechanism that controls directional migration and specifies the relative positions of the different cell types within the intestinal epithelium.

The Wnt signaling pathway plays a central role in the intestinal epithelium (reviewed in Bienz and Clevers, 2000; Kinzler and Vogelstein, 1996). The key event in this signaling pathway is the stabilization of β-catenin and its interaction with TCF transcription factors within the nucleus. Cytosolic levels of β-catenin are tightly regulated. In the absence of Wnt signals, a dedicated complex of proteins including APC, axin, and GSK3-β phosphorylates β-catenin, resulting in its ubiquitination and degradation by the proteasome. Signaling by Wnt factors blocks the activity of the destruction complex. β-catenin is stabilized and travels to the nucleus where it interacts with TCF transcription factors to drive the transcription of target genes (reviewed in Bienz and Clevers, 2000; Polakis, 2000)

Mutational activation of β-catenin/TCF in intestinal epithelial cells leads to polyp formation, the first morphological alteration that ultimately results in colorectal cancer (CRC) (reviewed in Fodde et al, 2001; Kinzler and Vogelstein, 1996). Mice deficient for the Tcf-4 transcription factor completely lack proliferative cells in the fetal small intestinal epithelium (Korinek et al., 1998). These findings suggest that β-catenin/TCF signaling is essential for maintaining the proliferative/undifferentiated state of intestinal epithelial cells, a notion elaborated in the accompanying paper (van de Wetering et al, 2002 [this issue of *Cell*]).

Eph receptors represent the largest subfamily of receptor tyrosine kinases. Based on their ligand binding specificity, these receptors are grouped into two subclasses. EphA receptors bind A-type ephrins, while EphB subfamily members bind B-type ephrins (reviewed in Flanagan and Vanderhaeghen, 1998; Frisen et al., 1999). The interactions between Eph receptors and ephrin ligands involve direct cell-to-cell interactions and frequently result in repulsion. Indeed, Eph-ephrin signaling provides repulsive clues in a wide range of developmental phenomena including axon pathfinding, the migration of neural crest cells, and boundary formation between segmented structures such as the rhombomeres (reviewed in Wilkinson, 2001; Holder and Klein, 1999; Robinson et al., 1997). In the latter developmental

[5]Correspondence: h.clevers@azu.nl
[6]Present address: Hubrecht Laboratory, Center for Biomedical Genetics, Uppsalalaan 8, 3584 CT Utrecht, The Netherlands.

system, Ephs and ephrins are expressed in complementary segments. It has been demonstrated that bidirectional signaling between receptors and ligands at the edge of even and odd rhombomeres is required to maintain the boundary between compartments (Xu et al., 1999; Mellitzer et al., 1999).

Here, we provide evidence that β-catenin/TCF signaling in the small intestine determines cell positioning along the crypt axis by controlling the expression of EphB and ephrinB genes.

## Results

### EphB2/EphB3 and their Ligand Ephrin-B1 Are Inversely Controlled by β-Catenin/TCF Signaling

As described in the accompanying paper (van de Wetering et al, 2002), we have performed a comprehensive analysis of the genetic program controlled by the β-catenin/TCF signaling pathway in CRC cells. Briefly, we found that genes downregulated by dominant-negative versions of TCF in CRC cell lines were physiologically expressed by the proliferative cells within the crypts. By contrast, genes that were upregulated upon the inhibition of β-catenin/TCF were expressed in differentiated cells of the intestinal epithelium.

Among the 120 cDNAs whose levels dropped upon inhibition of the β-catenin/TCF-mediated transcription, we noticed the EphB2 and EphB3 receptors. Furthermore, their ligand ephrin-B1 was among the 115 genes upregulated upon inhibition of β-catenin/TCF. We confirmed these data by Northern blot analysis (Supplemental Figure S1 available at http://www.cell.com/cgi/content/full/111/2/251/DC1).

In the small intestine of *E18* embryos, Tcf-4 expression is mainly confined to the rapidly proliferating, multipotent progenitor cells of the intervillus pockets (Korinek et al., 1998). As we demonstrated for other β-catenin/TCF target genes (van de Wetering et al., 2002 [this issue of *Cell*]), the expression domain of EphB2 and EphB3 is restricted to these proliferative areas (Supplemental Figure S1 available at above URL). However, the expression of both receptors was undetectable in the small intestines of *Tcf-4* deficient mice (Supplemental Figure S1 available at http://www.cell.com/cgi/content/full/111/2/251/DC1). This result provides further support for a role of β-catenin/TCF in controlling EphB2/-B3 expression in the intestine.

### EphB Receptors Control Actin Cytoskeleton Remodeling and Focal Adhesion Distribution in CRC Cells

In order to evaluate the function of the EphB2/-B3 RTKs in intestinal epithelial cells, we stimulated Ls174T cells with soluble ephrin-B1 to induce receptor activation (Figure 1). When seeded onto laminin, these cells spread, exhibiting numerous membrane protrusions resembling pseudopodia (Figure 1A, black arrowheads). A rapid change in morphology was induced by adding clustered soluble ephrin-B1/Fc recombinant ligand (Figure 1B). Within 20 minutes, the cells rounded up, yet recovered their original morphology after 2 hr (not shown).

Eph receptors control cell shape and migration through remodeling of the actin cytoskeleton (reviewed in Kullander and Klein, 2002). In spread Ls174T cells, actin is mainly organized into polymerized bundles that extend to focal contacts shaping membrane protrusions (Figures 1D and 1F, white arrowheads). Ephrin-B1 treatment recruited polymerized actin to the cell cortex (Figure 1E). Actin dynamics are essentially under the control of Rho, Rac, and Cdc42. The regulation of the activity of these three small GTPases is a well-characterized phenomenon in Eph-mediated axon repulsion and neuronal growth cone collapse (Kullander and Klein, 2002; Schmucker and Zipursky, 2001). The rounded morphology of CRC cells challenged with ephrin-B1 correlated with a decreased in Rac activity (Figure 1G, upper image).

Another hallmark of Eph/ephrin signaling is the regulation of cell-to-matrix adhesion (reviewed in Kullander and Klein, 2002; Wilkinson, 2001). In Ls174T cells, focal points of adhesion to the matrix were readily detectable with antibodies against the autophosphorylated form of focal adhesion kinase ($pY^{397}$-FAK) within the lamellipodia and cell extensions (Figures 1H–1K, white arrowheads). Ephrin-B1 treatment inhibited FAK (Figure 1P, left images), while the cells had not contracted yet (Figures 1L and 1M, empty arrowheads). FAK inhibition was confirmed by measuring the phosphorylation status of Paxillin, a FAK substrate (Schaller and Parsons, 1995) (Figure 1P, right images). FAK activity recovered after 10 minutes of stimulation with Ephrin-B1 (Figure 1P). However, active FAK localized to larger, mature focal adhesions underneath the cell body (Figure 1O, white arrowheads).

These results suggest that challenging intestinal cells with ephrin-B1 resulted in a cellular response reminiscent of that observed during cell contraction or axon repulsion mediated by Eph and ephrins in other cellular models.

### EphB2/-B3 and Ephrin-B1 Are Expressed in Complementary Domains in the Intestinal Epithelium of Newborn Mice

In the small intestine of newborn mice, EphB2 was expressed in the intervillus pockets of the epithelium (Figure 2A). Its expression domain coincided with that of Ki67, a proliferation marker (Figure 2C). This cell population also expressed EphB3 receptor in a largely overlapping pattern (Figures 2D and 2F). The EphB2 and EphB3 receptors bind all ephrin-B ligands: ephrin-B1, B2, and B3 (Brambilla et al., 1996, 1995; Gale et al., 1996). No expression of ephrin-B2 or ephrin-B3 was detected (not shown). However, ephrin-B1 was highly expressed by all epithelial cells excluding those localized at the bottom of intervillus pockets (Figure 2G). Double immunostaining demonstrated that cells at the periphery of the intervillus pockets coexpressed EphB2 receptor and ephrin-B1 ligand (Figure 2H, white arrowheads), while cells at the center of the pockets stained almost exclusively for the receptor (Figure 2H, empty arrowheads). A similar pattern was observed for EphB3 versus ephrin-B1 (not shown).

### EphB2 and EphB3 Establish a Boundary between Proliferative and Differentiated Cells

We then examined the intestines of neonatal mice deficient for EphB2 and/or EphB3. While the gross morphology of the intestines of *EphB2* or *EphB3* null animals

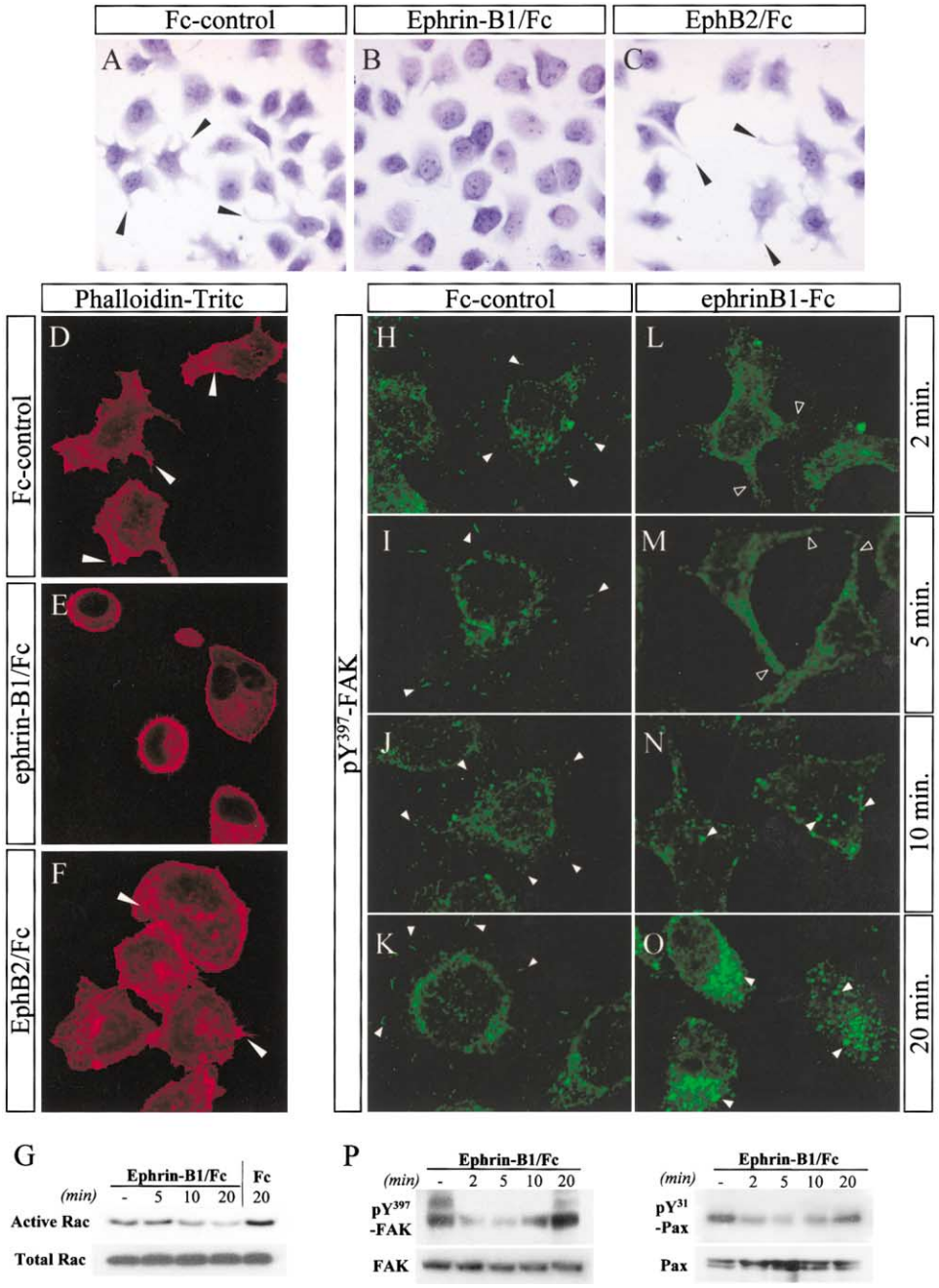


Figure 1. Activation of the EphB Receptors in Ls174T Cells Induces Actin Cytoskeleton and Focal Adhesion Remodeling

(A–F) Ls174T cells were treated with crosslinked IgG (Fc control, A and D), ephrin-B1/Fc fusion protein (B and E), or EphB2/Fc fusion protein (C and F). After 20 minutes, cells were fixed and stained with hematoxylin/eosine (A, B, and C) or with phalloidin-TRITC (D, E, and F). Black arrowheads indicate examples of cytoplasmic protrusions emanating from control cells. Actin is recruited from the stress fibers and speckles (white arrowheads) to the cortex upon addition of ephrin/Fc ligand. Representative fields are shown. Each of the fluorescent images represents equivalent projections taken under a confocal microscope.

(G) Active GTP-bound Rac was precipitated from lysates of LS174T using PAK1 Rac binding domain coupled to agarose (upper image). Cells were challenged with ephrin-B1/Fc for the indicated time points or with Fc control (IgG) for 20 minutes. Cell lysates showed equivalent total amounts of Rac (lower image).

(H–O) Localization of active FAK upon addition of crosslinked ephrin-B1/Fc fusion protein (L–O) or control IgG (H–K). Active FAK was detected at the indicated times using antibodies raised against the autophosphorylated tyrosine 397. Examples of pY397-FAK staining on focal adhesion are indicated with white arrowheads. Empty arrowheads point to cell expansions devoid of active FAK upon stimulation with ephrin-B1/Fc.

(P) Detection of pY397-FAK on cell lysates upon EphB stimulation with soluble ephrin-B ligand for the indicated time points (upper image, left). Inhibition of FAK activity coincides with the dephosphorylation of the FAK substrate paxillin (upper image, right). Total amounts of FAK and paxillin in the same lysates are shown in the lower images.

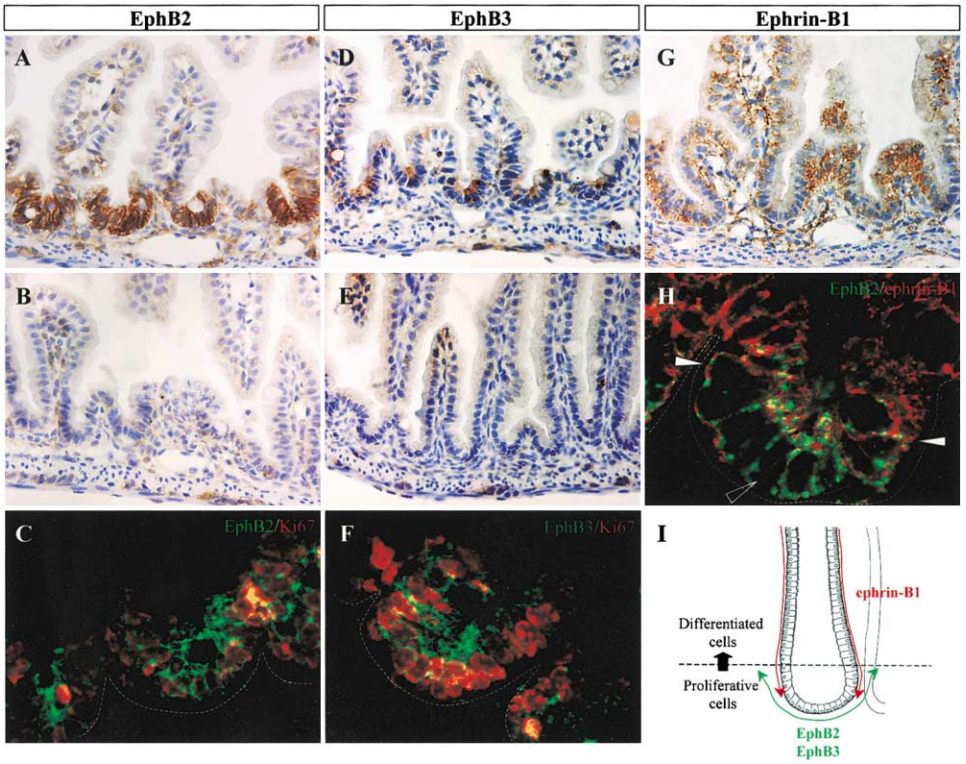


Figure 2. Expression Pattern of EphB2, EphB3, and Ephrin-B1 in the Small Intestine of Neonatal Mice

(A–F) EphB2 (A) and EphB3 (D) are expressed in the intervillus pockets of newborn animals. Antibody specificity is demonstrated by the lack of staining in equivalent sections from EphB2 (B) or EphB3 (E) homozygous null littermates. Double immunodetection of EphB2 (C, green labeling) or EPHB3 (F, green labeling) with Ki67 (red labeling) show that the receptors expression domains are restricted to proliferative cells.

(G) Staining of ephrin-B1 in neonatal intestine.

(H) Double immunostainings of EphB2 (green labeling) and ephrin-B1 (red labeling). Cells that border the intevillus pockets (white arrowheads) coexpress EphB2 and ephrin-B1, while cells at the bottom of the pockets stain almost exclusively for EphB2 (empty arrowheads). Dotted line depicts the round shape of the proliferative pockets.

(I) Schematic representation of the expression domains of the EphB2, EphB3, and their ligand ephrin-B1 in neonatal small intestine. EphB2 and EphB3 expression is restricted to the cells in the intervillus regions while ephrin-B1 is expressed in a complementary pattern by the adjacent cells in the villus. Proliferative cells bordering the intervillus pockets coexpress receptors and ligand.

was comparable to that observed in their heterozygous littermates (not shown), the shape and position of the intervillus pockets were disturbed in mice deficient for both receptors (*EphB2*$^{-/-}$ *EphB3*$^{-/-}$). In *EphB2*$^{-/-}$/*EphB3*$^{+/-}$ littermates (Figure 3A, inset), the intervillus pockets adopted the classical U-shaped morphology. In contrast, *EphB2*/*EphB3* double-deficient animals showed V-shaped pockets (Figure 3B, inset) that were not properly aligned along the intestinal wall (Figure 3B). The anatomy of the villus was normal.

Undifferentiated cells in the intervillus pockets stain for the nuclear Ki67 proliferation antigen, while differentiated enterocytes express the intestinal form of the Fatty Acid Binding Protein (FABP-i). In *EphB2* or *EphB3* single mutant mice, no differences in the distribution of the cell populations were observed when compared with their heterozygous littermates (Supplemental Figure S2 available at http://www.cell.com/cgi/content/full/111/2/251/DC1). *EphB2*$^{-/-}$/*EphB3*$^{+/-}$ mice also appeared normal. Ki67-positive cells were restricted to the intervillus regions at the bottom of the mucosa, while FABP-i expression started at the positions immediately above the proliferative area and extended along the villus (Figures 3C and 3E). A boundary between both cell populations was evident (Figure 3E, dashed lines). In *EphB2*/*EphB3* double-mutant mice, the boundary between the proliferative and the differentiated cells was largely absent. In the intervillus pockets, FABPi-expressing cells intermingled with the resident Ki67-positive cells (Figures 3D and 3F, white arrowheads). Ki67-positive cells were no longer restricted to the pocket region, but penetrated the villus domain, which is normally occupied exclusively by differentiated cells (Figures 3D and 3F, black arrowheads). We concluded that the concerted expression of EphB2 and EphB3 positions cell populations within the neonatal intestinal epithelium. We hypothesize that the interaction between EphB receptors on proliferative cells with their ligand ephrin-B1 on adjacent differentiated cells restricts cell intermingling.

### The Adult Mouse Intestine Shows a More Complex Pattern of EphB/Ephrin Expression

The overall structure of the adult small intestine is comparable to, yet more complex than that of the neonatal

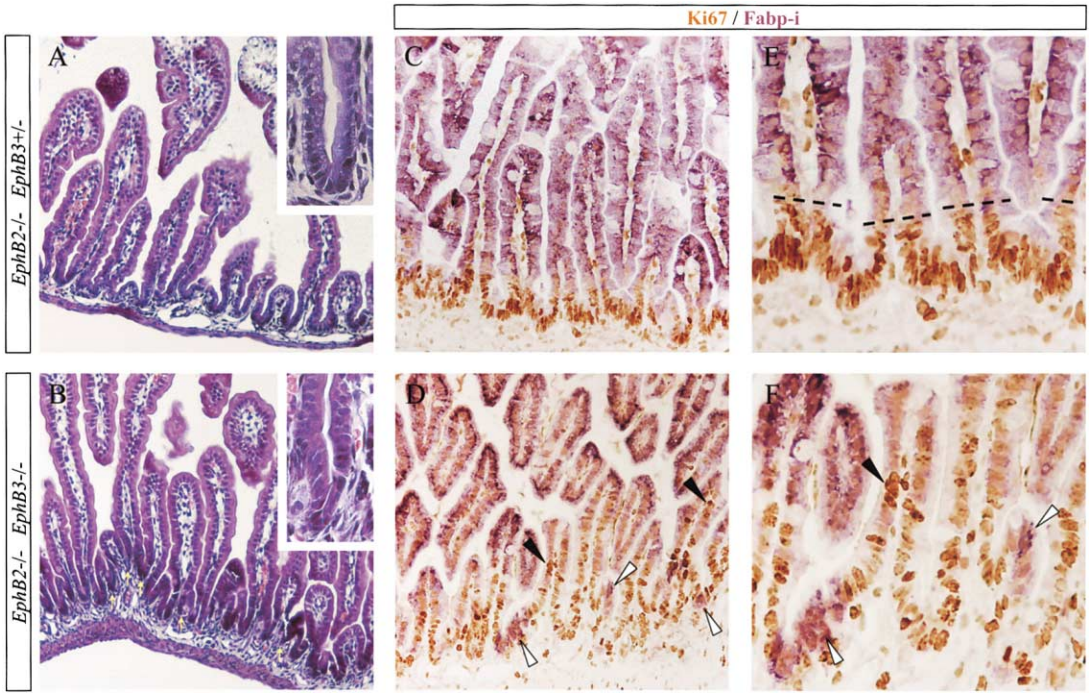


Figure 3. EphB2 and EphB3 Restrict Cell Intermingling in the Newborn Intestinal Epithelium

(A and B) Representative sections of the small intestine of *EphB2*$^{-/-}$/*EphB3*$^{+/-}$ (A) or *EphB2*$^{-/-}$/*EphB3*$^{-/-}$ (B) newborn animals stained with hematoxylin/eosine. Crypts are not properly aligned in double-mutant mice (arrows). Insets show the V-like morphology adopted by the intervillus regions in *EphB2*$^{-/-}$/*EphB3*$^{-/-}$ animals compared with the normal U-shape in control animals.

(C–F) Double labeling of proliferative cells (Ki67 positive, brown precipitate) and differentiated cells (I-Fabp positive, purple precipitate) in the small intestine of *EphB2*$^{-/-}$/*EphB3*$^{+/-}$ (C and E) or *EphB2*$^{-/-}$/*EphB3*$^{-/-}$ (D and F) newborn animals. In *EphB2*$^{-/-}$/*EphB3*$^{-/-}$ animals, differentiated cells (white arrowheads) and proliferative cells (black arrowheads) intermingle. Dotted lines depict the sharp boundary between the proliferative and the differentiated areas in control animals.

intestine. During the first two weeks of life, the postnatal intervillus pockets invaginate to form the crypts. This process culminates around the suckling/weaning transition, when the crypts acquire their mature structure. The adult crypt of Lieberkühn contains stem cells around positions 4–6 near the base, giving rise to a transient population of proliferating cells. These cells migrate toward the villus to become cell cycle arrested at the crypt-villus junction where they initiate differentiation. Paneth cells follow a downward migration path to occupy the bottom most positions in the crypt immediately below the putative stem cell zone.

The expression pattern of the EphB/ephrin-B system reflected this increased complexity (Figure 4). EphB2 was expressed throughout the proliferative compartment, peaking at positions 4–6, while its expression decreased in a gradient toward the top of the crypts (Figures 4C and 4D). The Ki67-positive cells that intercalate between Paneth cells at the bottom of the crypts ("crypt base columnar cells") stained strongly for EphB2 (Figure 4D, arrows; and Figure 4K, white arrowheads) yet lysozyme-positive Paneth cells were devoid of staining (Figure 4J, empty arrowheads). EphB3 expression was restricted to all cells located below the putative stem cell position (Figures 4A and 4B), although weak EphB3 staining could be detected in precursors located in the stem cell zone. Both Paneth (Figures 4M and 4N, empty arrowheads) and crypt base columnar cells (Figures 4M and 4N, white arrowheads) expressed EphB3.

High levels of ephrin-B1 and ephrin-B2 were detected at the crypt-villus junction. Their expression decreased gradually toward the bottom of the crypt (Figures 4E–4H). Thus, proliferative cells in the crypt coexpressed EphB2 receptors and their ligands in an inverse, position-dependent pattern. Differentiated cells above the first third of the villus showed little expression of ephrin-B1 or ephrin-B2 (Figures 4E and 4G, arrows). No expression of ephrin-B3 was detected in the small intestine (not shown).

### EphB3 Controls the Positioning of Paneth Cells

The overall structure of the adult epithelium was normal in single EphB2 and EphB3 mutant mice. However, *EphB3* homozygous null mice exhibited striking defects in the localization of Paneth cells, which were randomly distributed throughout the crypt (Figure 5B). Based upon granule size, many mislocalized Paneth cells were precursor cells. However, even fully mature Paneth cells were evident at the crypt-villus junction (Figure 5B, arrow). Lysozyme staining confirmed these observations (Figures 5C–5H). In *EphB3* and double *EphB2*/*EphB3* null animals, Paneth cells were evident throughout the crypt. We noticed that many mispositioned Paneth cells released their granules to the gut lumen (Fig-

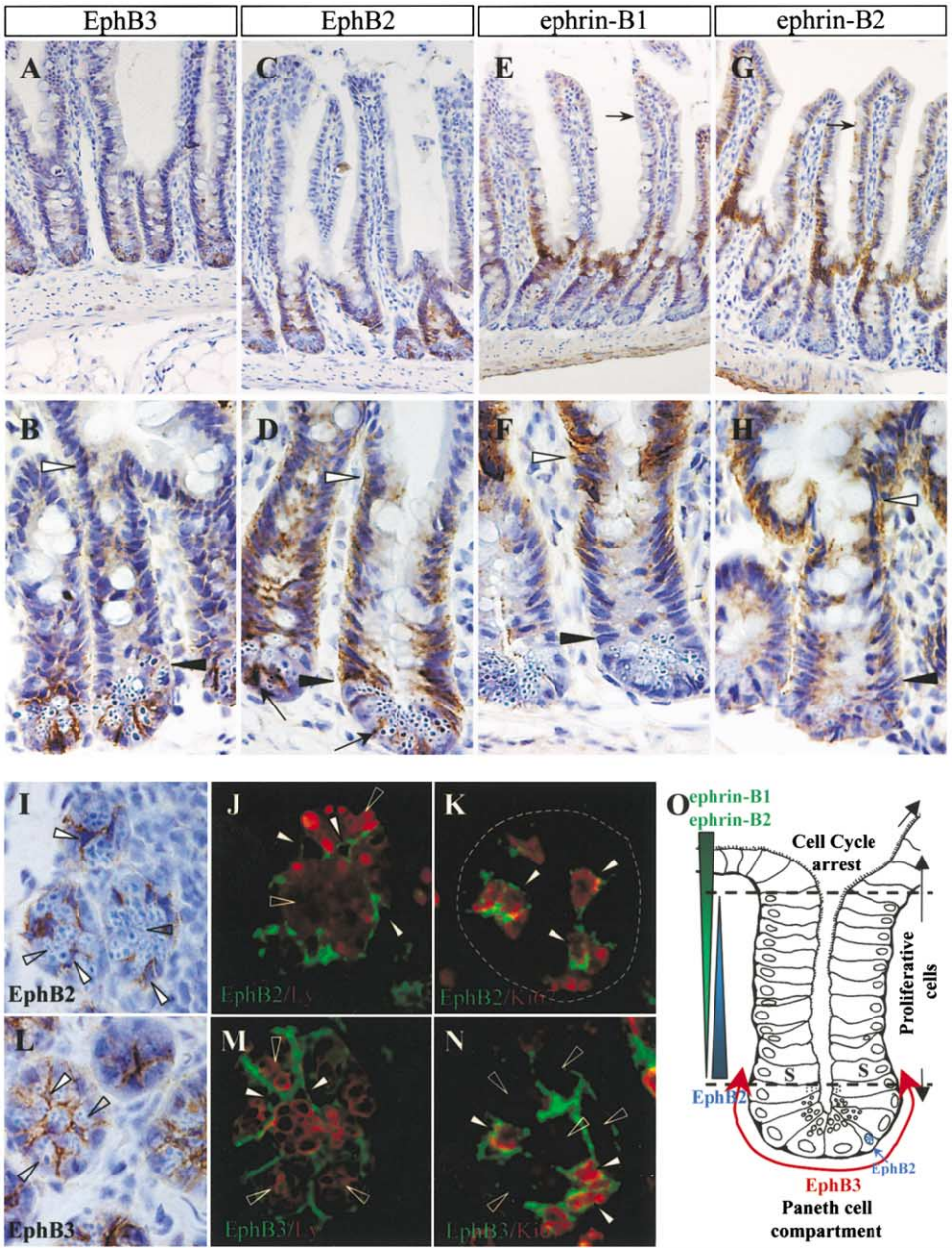


Figure 4. Expression Pattern of EphB2, EphB3, Ephrin-B1, and Ephrin-B2 in the Adult Small Intestine

(A–H) Immunodetection of EphB3 (A and B), EphB2 (C and D), ephrin-B1 (E and F), and ephrin-B2 (G and H) proteins in sections from the jejunum of adult (>7 weeks) mice. The arrow in (D) points to an EphB2 positive crypt base columnar cell. Black arrowheads indicate the boundary between the Paneth cell compartment and the proliferative compartment. White arrowheads point to the crypt-villus junction. Note that Paneth cells are easily recognizable by the presence of bright apical granules. Arrows in (E) and (G) indicate low levels of ephrin-B ligands in cells at the top of the villus.

(I–N) Expression of EphB2 (I-K) and EphB3 (L-N) in cells that localize at the bottom of the crypts. Stainings were performed on intestinal samples cut through the crypt base. Note that crypt base columnar cells (white arrowheads) appear as small cells spread between Paneth cells (empty arrowheads). Dotted lines indicate the perimeter of the crypt.

(O) Schematic representation of the expression gradients of EphB2, EphB3, and their ephrin ligands in the adult small intestinal crypts. Arrows show the direction of migration flow. S indicates the putative stem cell position.

ure 5B, inset). As a result, they were rarely detected on the villus. This altered localization was evident throughout the small intestine and represents a fully penetrant phenotype in *EphB3*$^{-/-}$ animals (n = 13). Limited scattering was observed in *EphB3*$^{+/-}$ mice (Figures 5E and 5G, white arrowheads), suggesting some degree of haploinsufficiency. No such defects were found in *EphB2* null mice (Figure 5D).

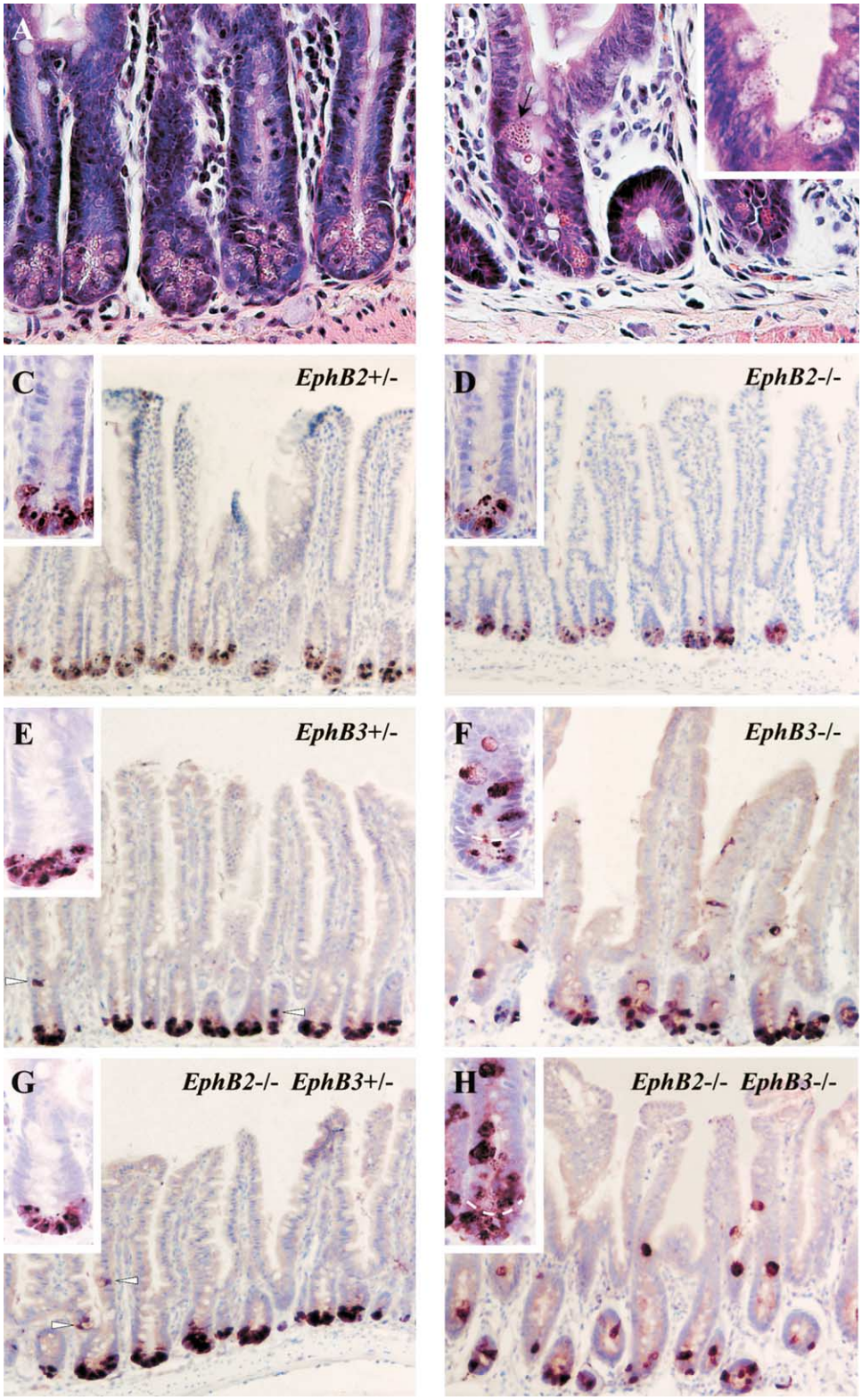


Figure 5. EphB3 Restricts the Localization of the Paneth Cells to the Bottom of the Crypts

(A and B) Hematoxylin/eosine staining of representative jejunal crypts of *EphB3*$^{+/-}$ (A) or *EphB3*$^{-/-}$ (B) adult (>7 weeks) mice. The arrow points to a morphologically mature Paneth cell mispositioned in the upper crypt region (B). Inset (B) shows Paneth cells at the villus releasing their apical granules to the lumen.

(C–H) Immunodetection of Paneth cells using an anti-lysozyme antibody in sections from the jejunum of *EphB2*$^{+/-}$ (C), *EphB2*$^{-/-}$ (D), *EphB3*$^{+/-}$ (E), *EphB3*$^{-/-}$ (F), *EphB2*$^{-/-}$/*EphB3*$^{+/-}$ (G), and *EphB2*$^{-/-}$/*EphB3*$^{-/-}$ (H) animals. Insets show representative crypts from each of the genotypes analyzed. White dashed lines depict the expected Paneth cell/proliferative cell boundary in *EphB3* null mice. Stainings were visualized with Vector-Vip substrate (purple precipitate) and counterstained with hematoxylin.

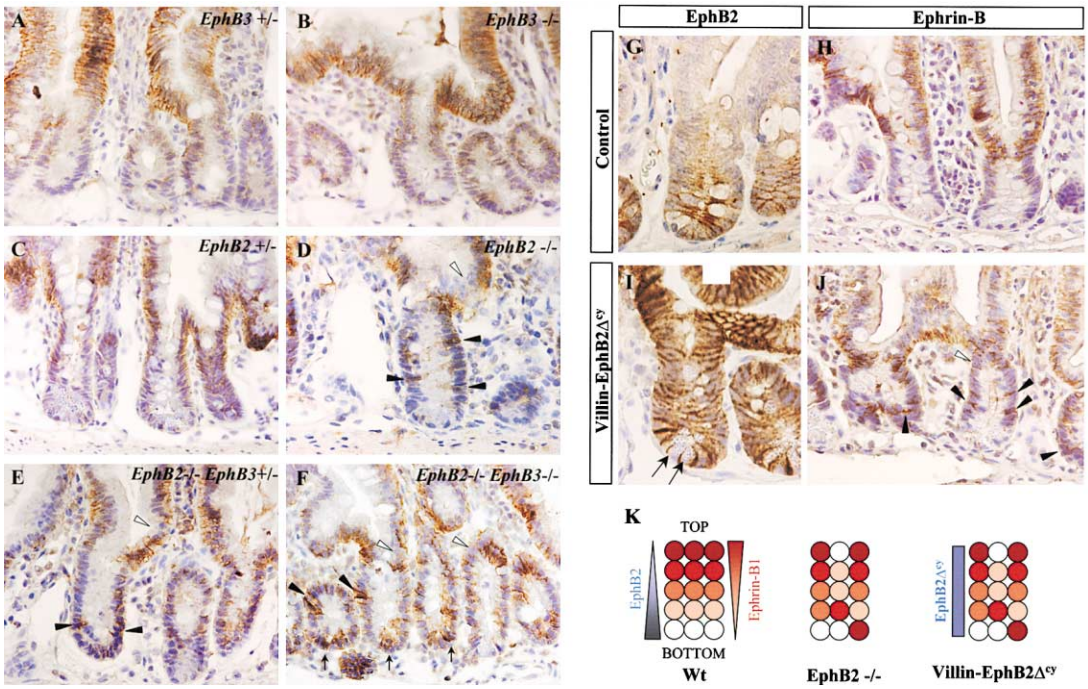


Figure 6. Aberrant Positioning of Ephrin-B Expressing Cells in the Small Intestine of *EphB2/EphB3* Deficient Animals and Villin-EphB2$\Delta^{cy}$ Transgenic Mice

(A–F) Ephrin-B immunostaining in distal duodenum/proximal adult jejunum samples using a Pan anti-ephrin antibody. Cells expressing high levels of ephrin-B that are scattered along the crypt are indicated with black arrowheads. White arrowheads point to clusters of cells showing reduced levels of ephrin-B at the crypt-villus junction. Ephrin-B positive cells also occupy the Paneth cell region in *EphB2*$^{-/-}$/*EphB3*$^{-/-}$ animals (arrows).

(G–J) Analysis of villin-EphB2$\Delta^{cy}$ transgenic animals.

(G and I) Immunostaining using an antibody directed against the extracelullar domain of EphB2 in wild-type (G) or villin-EphB2$\Delta^{cy}$ transgenic (I) jejunal crypts. Arrows indicate Paneth cells expressing the EphB2$\Delta^{cy}$.

(H and J) Ephrin-B expression pattern in wild-type (H) or villin-EphB2$\Delta^{cy}$ transgenic mice (J). Black arrowheads indicate mispositioned cells expressing high levels ephrin-B. White arrowheads point to cells showing low levels of ephrin-B located at the crypt-villus junction.

(K) Schematic representation of the phenotypes found in EphB2 deficient animals or villin-EphB2$\Delta^{cy}$ transgenics. In the presence of an increasing gradient of EphB2 receptor, ephrin-B positive precursors organize from top to bottom following a reverse gradient of Ephrin-B1 expression (left image). Ablation of EphB2 results in an almost random localization of precursors expressing different levels of ephrin-B1 along the axis (middle image). A similar phenotype results from a homogeneous expression along the crypt-villus axis of an EphB2 receptor lacking the cytoplasmic domain.

### Disruption of EphB2 Gradient Alters Positioning of Ephrin-B Positive Cells

Proliferative cells residing between the putative stem cell position and the crypt-villus junction represent precursors at different stages of commitment (reviewed in Stappenbeck et al., 1998; Potten and Loeffler, 1990). We have shown that the expression levels of EphB2 and ephrin-B in each of these precursors inversely depend on their positions along the crypt axis (Figure 4). Therefore, the relative level of receptor or ligands represents a positional marker suitable for tracking alterations in the allocation of this cell population. In control animals, ephrin-B expression increased gradually toward the crypt-villus junction (Figures 4F and 4H; Figures 6A–6C). This gradient was severely disturbed in EphB2/-B3 double-mutant animals (Figure 6F). Cells staining strongly for ephrin-B occurred throughout the crypts (Figure 6F, black arrowheads). Conversely, cells showing very low levels of ephrin-B were present at the crypt-villus junction (Figure 6F, white arrowheads). A less extensive disturbance was present in *EphB2* null mice carrying one or two wild-type *EphB3* alleles (Figures 6D and 6E). *EphB3*$^{-/-}$ mice showed a wild-type pattern of ephrin-B expression (Figures 6A and 6B).

These observations suggested that complementary expression of EphB receptors and ligands in individual cells restrict their potential positions along the crypt axis. We sought further evidence to support this scenario by experimental manipulation of the EphB expression gradient. This was achieved through transgenic expression of a dominant-negative version of the EphB2 receptor lacking the intracellular domain (EphB2-$\Delta^{cy}$). Similar truncated receptors have been used previously to interfere with Eph function (Xu et al. 1995). The villin promoter (Pinto et al. 1999) directed uniform, high level expression of the transgene throughout the intestinal epithelium (Figure 6I; Supplemental Figure S3 available at http://www.cell.com/cgi/content/full/111/2/251/DC1). In these mice, precursor cells did not localize according to their ephrin-B levels, but were positioned randomly along the crypts (Figure 6J). Furthermore, a high proportion of Paneth cells was mispositioned in the transgenic animals (Supplemental Figure S3 available at above URL). These results implied that the receptor gradient

along the crypt axis is required for the correct positioning of ephrin-B expressing precursors.

### β-Catenin Accumulation in the Intestinal Epithelium Is Cell Non-Autonomous Process

In the accompanying paper (van de Wetering et al., 2002), we show that proliferative cells at the bottom of the colon crypts accumulate nuclear β-catenin. In the small intestine, nuclear β-catenin was evident in the bottom third of all crypts examined (Figures 7A–7D, white and blue arrowheads) while cells located above this region contained exclusively membrane β-catenin (Figures 7A–7D, empty arrowheads). Moreover, Paneth cells invariably contained high levels of nuclear β-catenin (Figures 7A–7D, blue arrowheads). Therefore, physiological β-catenin/TCF signaling occurs in the bottom most cells including the Paneth cells. We next asked whether this phenomenon is a cell autonomous process. Despite the extensive intermingling of cell types present in *EphB2/B3* mutant animals, nuclear β-catenin occurred only in cells at the bottom of the crypts (Figures 7E–7H, blue and white arrowheads), including Paneth cells (Figures 7E–7G, blue arrowheads). Paneth cells mispositioned above the first third of the crypt were invariably negative (Figures 7E–7G, arrows). Thus, nuclear accumulation of β-catenin in the small intestine is a cell non-autonomous process and depends on the position that cells adopt along the crypt-villus axis.

### EphB and Ephrin Expression Domains Are Compartmentalized in Colorectal Cancer

Nuclear β-catenin accumulates in a cell-autonomous fashion in CRC as the result of the mutational activation of the Wnt pathway. We next asked whether this pathological switch in the control of nuclear β-catenin also affects the distribution of cell types in the intestinal epithelium. *min* (*multiple intestinal neoplasia*) mice carry a truncated *APC* allele. Loss of the wild-type allele triggers the formation of a polyp (Figures 7I–7K, black arrowheads), which accumulates high levels of cytoplasmatic and nuclear β-catenin (Figure 7I). Polyps expressed high levels of EphB2 (Figure 7J) and EphB3 (not shown) but did not express ephrin-B ligands (Figure 7K). This observation further supports the notion that β-catenin/Tcf activity inversely controls the expression of Eph receptors and their ligands. The structure of the epithelium in the polyp areas is grossly disrupted by the overgrowth of APC mutant cells. Despite this aberrant morphology, a strict compartmentalization of EphB and ephrin-B expressing cells was evident. A layer of normal cells expressing ephrin-B ligands (Figure 7K, white arrowheads) surrounded EphB2-positive polyp cells, yet intermingling of the two cell populations was never observed.

## Discussion

In the accompanying paper (van de Wetering et al., 2002), we describe a comprehensive analysis of the genetic program controlled by β-catenin/TCF in CRC. The identification of EphB receptors and their ephrin ligands in the short list of β-catenin/TCF-controlled genes prompted the current study. Here we describe two aspects of EphB biology in the gut. First, we show that β-catenin and TCF inversely control the expression of EphB and ephrin-B genes. Second, we demonstrate that expression of EphB receptors is essential for the correct positioning of epithelial cells along the crypt/villus axis.

While the crypt/villus axis is anatomically well defined, the molecular mechanisms responsible for the induction and maintenance of this axis are unclear. We demonstrate that only those cells localized at the crypt base in the small intestine and colon accumulate nuclear β-catenin in a cell non-autonomous fashion. These observations strongly suggest the presence of a localized source of Wnt factors at the base of the crypts. Although several Wnt factors are known to be expressed in the developing gut (Lickert et al, 2001), such a localized source of Wnts remains hypothetical. Nevertheless, the temporal expression of receptors and ligands in the engineered CRC cells is recapitulated by their spatial expression domains in the small intestinal crypts: EphB expression is highest at the bottom of the crypt, close to the putative Wnt source, while ephrin-B expression peaks at the surface epithelium.

### A Model for EphB/Ephrin-B Mediated Cell Sorting in the Intestinal Epithelium

This study describes two effects of EphB mutations on cell positioning, i.e., on the localization of Paneth cells in small intestine crypts and on the allocation of the proliferative and differentiated cells along the crypt-villus axis. These two phenomena are discussed below.

Paneth cells are unusual in that they follow a downward migratory path in the crypt. They express high levels of EphB3, but are negative for EphB2. In *EphB3*, null mice Paneth cells no longer follow their downward migratory path. Interestingly, despite the fact that Paneth cells are quiescent differentiated cells, they accumulate nuclear β-catenin when they localize close to the putative Wnt source at the crypt base, yet this localization is not required for their maturation. Of note, the experimental depletion of Paneth cells does not cause any major abnormality in gut physiology (Garabedian et al., 1997).

Cells in the neonatal intervillus pockets coexpress EphB2 and EphB3. Single *EphB2* or *EphB3*-deficient mice display no phenotype in these proliferative pockets. In the *EphB2/EphB3* double mutants, the proliferative and differentiated cells intermingle. Importantly, some intervillus regions in the *EphB2/EphB3* double-deficient mice contain differentiated cells without an apparent altered localization of proliferative cells. This non-autonomous effect on the differentiated ephrin-B1 expressing cells cannot be explained simply as the result of the passive movement of differentiated cells to fill the gaps left by the proliferative cells. Rather, it suggests that the presence of the EphB receptors in wild-type proliferative regions actively restricts the migration of differentiated cells. This situation is reminiscent of the establishment of segment boundaries in the developing hindbrain where bidirectional signaling occurs between Eph and ephrin expressing populations at the edge of odd and even rhombomeres (Xu et al., 1999; Mellitzer et al., 1999). We often observed groups of mispositioned cells rather than extensive individual intermingling, suggesting that certain adhesive properties are retained in cells with similar identities.

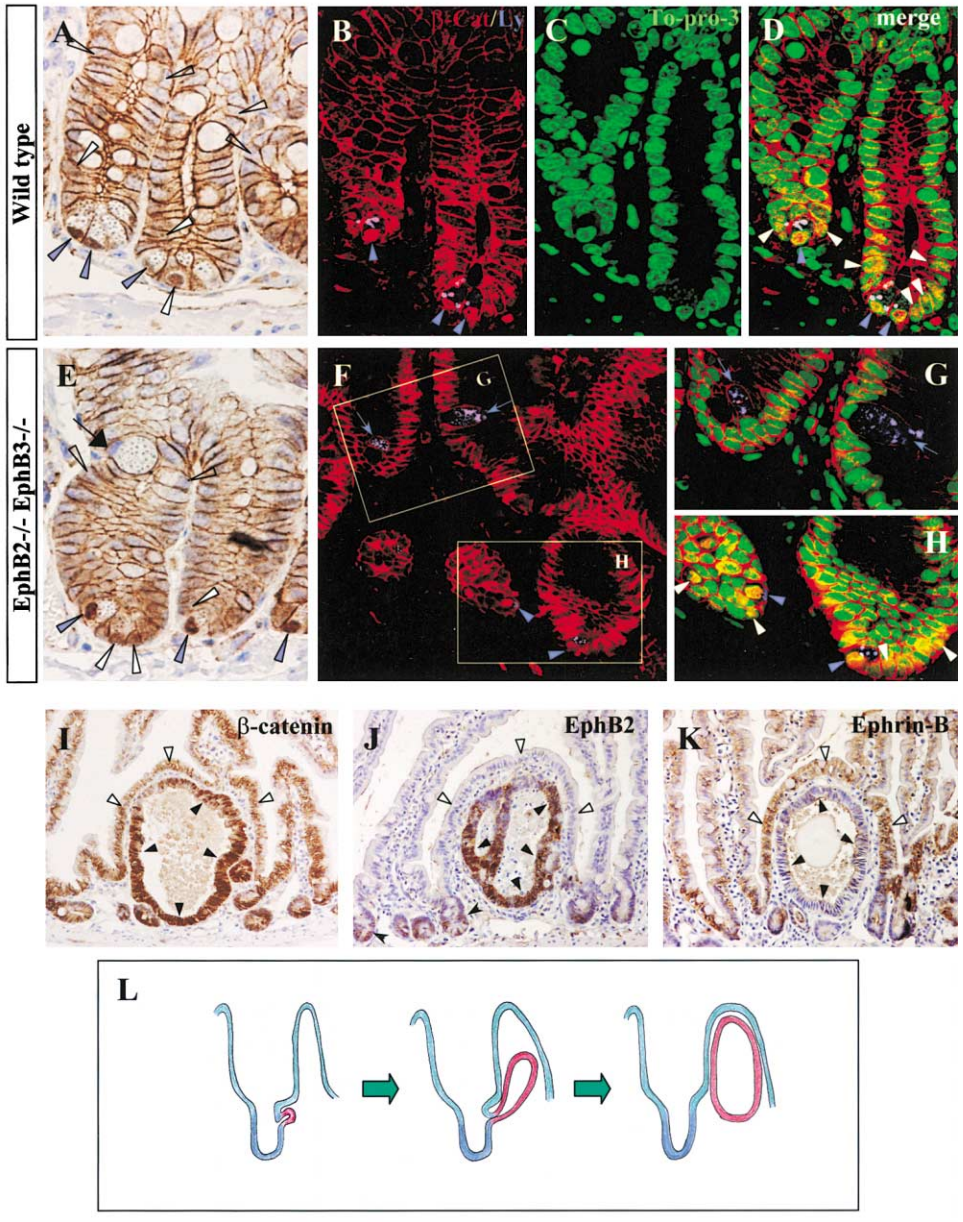


Figure 7. β-Catenin Accumulates in the Nucleus of Cells at the Crypt Base in a Non-Autonomous Fashion

(A and E) β-catenin staining in crypts from wild-type animals (A) or EphB2/-B3 double deficient animals (E). Blue arrowheads point to Paneth cells at the crypt base showing high levels of nuclear β-catenin. White arrowheads indicate examples of cells without an apparent Paneth cell morphology that also appear positive for nuclear β-catenin staining. Empty arrowheads illustrate examples of cells above the first third of the crypt devoid of nuclear β-catenin. Arrow in (E) indicates a mispositioned Paneth cell at the top of the crypt.

(B–H) Double immunostaining for β-catenin (red) and lysozyme (blue) in wild-type (B–D) or EphB2/-B3 double-mutant animals (F–H). Nuclei were counterstained with To-pro-3 (green). Blue arrowheads show lysozyme positive cells that accumulate nuclear β-catenin at the crypt base. White arrowheads indicate nuclear β-catenin positive cells that do not express lysozyme. Blue arrows depict lysozyme positive cells at the villus devoid of nuclear β-catenin staining. (G) and (H) are merged magnifications of (F). Images are representative confocal sections of jejunal crypts.

(I–K) Analysis of the expression patterns of β-catenin (I), EphB2 (J), and ephrin-B ligands (K) in polyps from Min mice. Polyp cells (black arrowheads) accumulate high levels of β-catenin. Accordingly, they overexpress EphB2 receptor but do not express ephrin-B ligands. The layer of normal cells that surrounds the polyps (white arrowheads) shows the reverse pattern of EphB2 and ephrin-B. Note the expression of EphB2 in normal crypts around the polyp areas (J, arrows).

(L) Polyp formation in the small intestine as described in Oshima, et al. 1997. Blue depicts the crypts and green the villus. Mutant APC cells (red) invaginate around the crypt-villus junction and migrate into the adjacent villus.

The proliferative zone of the adult crypt is a much more elaborate structure than the intervillus pocket of the neonate. Each position along the adult crypt axis is characterized by different levels of EphB and ephrin-B molecules. Our data indicate that EphB restricts the potential positions adopted by cells expressing different

levels of ephrin-B. In the absence of Eph signaling, cells otherwise positioned at the bottom of the proliferative zone localize at the crypt-villus junction. Many of the cells with high levels of ephrin-B can relocalize from the crypt-villus junction to the bottom of the crypts. The latter observation implies that receptors as well as ligands may transduce repulsive signals. Moreover, since these cells relocate close to the putative Wnt source at the bottom of the crypts but still express high levels of ephrin-B, we hypothesize that they may represent precursors that have been already committed toward cell fate and, therefore, are not immediately reprogrammed.

Similar expression gradients of Eph receptors and ephrin ligands have been shown to set up the topographic maps of neuronal connections. During chick development, the tectum shows a gradient of ephrin-A ligands increasing from anterior to posterior. As a result, temporal axons from the retina with high EphA3 project to the anterior tectum, whereas nasal axons with lower levels of EphA3 target the posterior tectum (reviewed in Wilkinson, 2000, 2001). A similar mechanism can be envisioned in the intestine where cells expressing high levels of EphB2/B3 receptors avoid being surrounded by cells expressing high levels of the ligand and vice versa. Note that in this model, cells cannot migrate downward: they are excluded from the positions immediately below due to their higher expression of ephrin-B1. This mechanism may ensure the unidirectional migration in the crypt. On the other hand, the absence of ephrin-B ligands and the high levels of EphB3 receptor in Paneth cells results in the sorting of this particular lineage to the bottom of the crypts. Further support for this double-restriction model comes from the analysis of EphB2-$\Delta^{cy}$ transgenic animals. In these mice, the truncated receptor exerts a dominant-negative effect on EphB positive cells (cells at the crypt base, i.e., Paneth cells) yet it is still able to activate ephrin-B ligands. However, the sorting of precursors expressing high levels of ephrin-B (which are EphB-negative) is also impaired. In these mice, ephrin-B positive precursors are surrounded by cells expressing equivalent amounts of EphB2-$\Delta^{cy}$ and, therefore, homogenous rather than graded signaling occurs. Under these circumstances, ephrin-B positive cells may experience equivalent restrictions in their possible migratory paths and adopt random positions.

### Definition and Stabilization of the Pattern in the Intestinal Epithelium

Unexpectedly, the intestine of *EphB2/EphB3* double-deficient newborn animals matures normally despite the disordered epithelial organization. Apparently, mispositioning of cells does not represent a major obstacle for the intestine to generate adult structures. We argue that β-catenin/TCF signaling couples cell positioning with cell proliferation, cell cycle arrest, and differentiation. These three latter processes appear unaffected in EphB mutant intestine. Accordingly, the pattern of nuclear β-catenin in EphB2/B3 null epithelium is identical to that of wild-type animals, and the crypt/villus axis remains essentially intact. As is the case for somites (Durbin et al., 1998) or hindbrain (Xu et al., 1995), EphB/Eprhrin interactions stabilize but do not define tissue patterning in the intestinal epithelium.

### Passive Migration Versus Active Repulsion in the Intestinal Epithelium

The migration of intestinal cells is believed to result from passive mechanisms (reviewed in Heath, 1996). First, the generation of cells in the crypts transmits a pressure along the crypt-villus axis. Second, gaps left by the extruded mature cells at the top of the villi are immediately reoccupied. As a result, epithelial cells attached to each other by cell-to-cell contacts are forced to migrate upward. We have demonstrated that EphB2 and EphB3 further refine this mechanism by establishing restrictions to this passive migration. Our results imply that epithelial organization is more plastic than expected. In the absence of EphB signaling, cells are positioned independently of the upstream migration flow.

Signaling by Eph receptors is only partially understood. The actin cytoskeleton reorganization induced by EphB activation on intestinal cells is reminiscent of that in growth cone repulsion (Shamah et al., 2001; Meima et al., 1997a , 1997b; Elowe et al., 2001). In our system, inhibition of Rac activity likely mediates the retraction of pseudopodia and membrane protrusions. Furthermore, Eph signaling in intestinal cells induces rearrangement of the focal adhesions. FAK activity is rapidly blocked, even before cells have started to contract. FAK inhibition is likely upstream of actin cytoskeleton remodeling. A similar effect on FAK activity has been reported for EphA2 activation (Miao et al, 2000). Newly generated focal adhesion complexes formed at the edge of the cells provide new adhesive contacts and thus direct cell movement (Horwitz and Parsons, 1999). Accordingly, inhibition of FAK reduces cell motility (reviewed in Parsons et al, 2000). Spatial regulation of FAK activity may restrict cell migration in the intestinal epithelium upon Eph-ephrin interaction.

### Is the Eph/Ephrin System Involved in Intestinal Tumorigenesis?

Polyps in the small intestine of Min mice develop as invaginations of the epithelial layer (Oshima et al, 1997 and Figure 7L). Groups of cells located around the crypt-villus junction form pockets that migrate inside the normal epithelium of the villus. These cells proliferate inside the mucosa as a disorganized mass that eventually give rise to a tumor. This abnormal migratory behavior is likely the outcome of the β-catenin/Tcf target gene program autonomously activated in APC mutant cells and results in a further compartmentalization of EPHB and ephrin-B expressing cells in the polyp areas. This observation does not imply a causal role for Eph signaling in polyp formation. Yet, it is intriguing that this initial outpocketing arises at the crypt-villus junction where APC-mutant cells that overexpress EphB receptors encounter the maximum threshold of ephrin-mediated repulsion. We speculate that the initial founding polyp cells, which express high levels of EphB receptors, migrate abnormally inside the villus to avoid the area of high ephrin-B expression at the top positions of the crypts. Analysis of $APC^{min}$ epithelium in an EphB deficient background will test this hypothesis.

## A Role for the Eph/Ephrin System in the Structure and Function of the Adult Tissues

Over the last two decades, developmental biology has focused on the elucidation of the signaling pathways that shape the embryo. More recently, it has been appreciated that such programs often play analogous roles in adult tissues. The β-catenin/TCF signaling pathway and the EphB/ephrin-B system in the adult intestine may be a prime example. The diversification of the Eph/ephrin family arises in vertebrates concomitantly with an increase in tissue and cell complexity. Several epithelia show continuous renewal in a pattern analogous to the intestine. Many other processes that take place in adult organs require precise cell allocation. EST database searches indicate that many cell types express Eph/ephrin family members. We speculate that the combinatorial expression of Eph receptors and ephrin ligands may define migration and positioning in a wide spectrum of adult tissues.

### Experimental Procedures

#### Expression Vectors

The villin-EPHB2-$\Delta^{cy}$ transgenic expression construct was engineered by fusing the Flag tag sequence plus a stop codon to a murine EPHB2 cDNA at amino acid 602, immediately downstream of the transmembrane domain. The resulting reading frame was cloned at the initiation codon of the Villin 9 Kb promoter (Pinto et al. 1999). An SV40 termination and poly-adenylation cassette was added downstream.

#### Cell Culture and Transfections

Ls174T cells were cultured in RPMI with 10% FCS. The T-REX system (Invitrogen) was used according to the manufacturer's instructions to generate doxycycline inducible DN-TCF-4 or DN-TCF-1 expressing cells (for more details see accompanying paper, van de Wetering et al, 2002).

#### Northern-Blotting

The following probes were used: EphB2 (nucleotides 2960 to 3771), EphB3 (nucleotides 3296 to 3708), and ephrin-B1 (nucleotides 2644 to 2897).

#### Induction of EphB/Ephrin-B Activity Using Recombinant Fc Fusion Proteins

Recombinant extracellular domains of the EphB2 receptor or ephrin-B1 ligand fused to the Fc fragments of the human immoglobulins were from R&D Systems, Inc. Human immunoglobulins or Fc-recombinant proteins were crosslinked using anti-Fc antibodies at 2:1 (Fc:antibody) molar ratio in PBS for 1 hr at room temperature. Ls174T cells were seeded at low density on to laminin-coated plates (2 μg/cm$^2$). After 12 hr, crosslinked IgG or Fc-recombinant proteins were added to at 5 μg/ml.

#### Mouse Lines

*EphB2* and *EphB3* null animals were previously described (Orioli et al., 1996; Henkemeyer et al., 1996.) *EphB2* and *EphB3* murine stocks were maintained on either 129SV/cp or outbred genetic backgrounds. *EphB2/EphB3* double knockouts were maintained on an outbred background. Mice were sacrificed for analysis by cervical dislocation. All procedures were performed in accordance with the protocols of the Samuel Lunenfeld Research Annex, the Canadian Council on Animal Care, and the Ontario Ministry of Agriculture.

#### Antibodies

The following antibodies were used. Goat anti-EphB2 (1:200; R&D systems), goat anti-EphB3 (1:100; R&D systems), goat anti-ephrin-B1 (1:400; R&D systems), goat anti-ephrin-B2 (1:200; R&D systems), goat anti-ephrin-B3 (1:100; R&D systems). Rabbit anti-ephrin-B1 (1:200; Santa Cruz; C-18) is pan-ephrin-B, Rabbit anti-Lysozyme (1:500; DAKO), mouse anti-Ki67 (1:100; Novocastra), rabbit anti-FABPi (a kind gift from Prof. J.I. Gordon; 1:800), and mouse anti-β-catenin (1:50; Transduction Labs). Antibodies against the phosphorylated forms of FAK and Paxillin were from Biosource International.

#### Tissue Sample Preparation and Immunohistochemistry

A detailed protocol of the immunohistochemical methods is provided as Supplemental Data available at http://www.cell.com/cgi/content/full/111/2/251/DC1.

#### Rho, Rac, and Cdc42 Pull-Down Assays

Active GTP-bound Rho was pulled-down using a GST-Rhotekin Rho binding domain fusion protein coupled to agarose (Upstate Biotechnology). GTP-bound Rac and cdc42 was pulled down using a GST-PAK1 fusion protein coupled to agarose (Upstate Biotechnology). The assay was performed according to the manufacturer's instructions.

#### Acknowledgments

We thank Prof. R. Klein, Prof. K. Artories, Prof. L.M. Matrisian, Prof. J.I Gordon, Dr. J. Fawcett, Dr. C. Bolós, Prof. D. Louvard, Prof. A.B. Leiter, and Dr. S. Robine for valuable reagents. E.B. and E.S. hold Marie Curie Fellowships. This research was supported by a grant from the Canadian Institute for Health Research (CIHR) to T.P. and J.T.H. H.C. is supported by grants from the Netherlands Cancer Foundation. T.P. is a Distinguished Scientist of the CIHR.

Received: February 4, 2002
Revised: September 5, 2002

### References

Bienz, M., and Clevers, H. (2000). Linking colorectal cancer to Wnt signaling. Cell *103*, 311–320.

Brambilla, R., Schnapp, A., Casagranda, F., Labrador, J.P., Bergemann, A.D., Flanagan, J.G., Pasquale, E.B., and Klein, R. (1995). Membrane-bound LERK2 ligand can signal through three different Eph-related receptor tyrosine kinases 12. EMBO J. *14*, 3116–3126.

Brambilla, R., Bruckner, K., Orioli, D., Bergemann, A.D., Flanagan, J.G., and Klein, R. (1996). Similarities and differences in the way transmembrane-type ligands interact with the Elk subclass of Eph receptors. Mol. Cell. Neurosci. *8*, 199–209.

Durbin, L., Brennan, C., Shiomi, K., Cooke, J., Barrios, A., Shanmugalingam, S., Guthrie, B., Lindberg, R., and Holder, N. (1998). Eph signaling is required for segmentation and differentiation of the somites. Genes Dev. *12*, 3096–3109.

Elowe, S., Holland, S.J., Kulkarni, S., and Pawson, T. (2001). Down-regulation of the Ras-mitogen-activated protein kinase pathway by the EphB2 receptor tyrosine kinase is required for ephrin-induced neurite retraction. Mol. Cell. Biol. *21*, 7429–7441.

Flanagan, J.G., and Vanderhaeghen, P. (1998). The ephrins and Eph receptors in neural development. Annu. Rev. Neurosci. *21*, 309–345.

Fodde, R., Smits, R., and Clevers, H. (2001). APC, signal transduction and genetic instability in colorectal cancer. Nat. Rev. Cancer *1*, 55–67.

Frisen, J., Holmberg, J., and Barbacid, M. (1999). ephrins and their Eph receptors: multitalented directors of embryonic development. EMBO J. *18*, 5159–5165.

Gale, N.W., Holland, S.J., Valenzuela, D.M., Flenniken, A., Pan, L., Ryan, T.E., Henkemeyer, M., Strebhardt, K., Hirai, H., Wilkinson, D.G., et al. (1996). Eph receptors and ligands comprise two major specificity subclasses and are reciprocally compartmentalized during embryogenesis. Neuron *17*, 9–19.

Garabedian, E.M., Roberts, L.J., McNevin, M.S., and Gordon, J.I. (1997). Examining the role of Paneth cells in the small intestine by lineage ablation in transgenic mice. J. Biol. Chem. *272*, 23729–23740.

Heath, J.P. (1996). Epithelial cell migration in the intestine. Cell Biol. Int. *20*, 139–146.

Henkemeyer, M., Orioli, D., Henderson, J.T., Saxton, T.M., Roder,

J., Pawson, T., and Klein, R. (1996). Nuk controls pathfinding of commissural axons in the mammalian central nervous system. Cell *86*, 35–46.

Holder, N., and Klein, R. (1999). Eph receptors and ephrins: effectors of morphogenesis. Development *126*, 2033–2044.

Horwitz, A.R., and Parsons, J.T. (1999). Cell migration--movin' on. Science *286*, 1102–1103.

Kinzler, K.W., and Vogelstein, B. (1996). Lessons from hereditary colorectal cancer. Cell *87*, 159–170.

Korinek, V., Barker, N., Moerer, P., van Donselaar, E., Huls, G., Peters, P.J., and Clevers, H. (1998). Depletion of epithelial stem-cell compartments in the small intestine of mice lacking TCF-4. Nat. Genet. *19*, 379–383.

Kullander, K., and Klein, R. (2002). Mechanisms and functions of eph and ephrin signalling. Nat. Rev. Mol. Cell Biol. *3*, 475–486.

Lickert, H., Kispert, A., Kutsch, S., and Kemler, R. (2001). Expression patterns of Wnt genes in mouse gut development. Mech. Dev. *105*, 181–184.

Meima, L., Kljavin, I.J., Moran, P., Shih, A., Winslow, J.W., and Caras, I.W. (1997a). AL-1-induced growth cone collapse of rat cortical neurons is correlated with REK7 expression and rearrangement of the actin cytoskeleton. Eur. J. Neurosci. *9*, 177–188.

Meima, L., Moran, P., Matthews, W., and Caras, I.W. (1997b). Lerk2 (ephrin-B1) is a collapsing factor for a subset of cortical growth cones and acts by a mechanism different from AL-1 (ephrin-A5). Mol. Cell. Neurosci. *9*, 314–328.

Mellitzer, G., Xu, Q., and Wilkinson, D.G. (1999). Eph receptors and ephrins restrict cell intermingling and communication. Nature *400*, 77–81.

Miao, H., Burnett, E., Kinch, M., Simon, E., and Wang, B. (2000). Activation of EphA2 kinase suppresses integrin function and causes focal-adhesion-kinase dephosphorylation. Nat. Cell Biol. *2*, 62–69.

Orioli, D., Henkemeyer, M., Lemke, G., Klein, R., and Pawson, T. (1996). Sek4 and Nuk receptors cooperate in guidance of commissural axons and in palate formation. EMBO J. *15*, 6035–6049.

Oshima, H., Oshima, M., Kobayashi, M., Tsutsumi, M., and Taketo, M.M. (1997). Morphological and molecular processes of polyp formation in Apc(delta716) knockout mice. Cancer Res. *57*, 1644–1649.

Parsons, J.T., Martin, K.H., Slack, J.K., Taylor, J.M., and Weed, S.A. (2000). Focal adhesion kinase: a regulator of focal adhesion dynamics and cell movement. Oncogene *19*, 5606–5613.

Pinto, D., Robine, S., Jaisser, F., El Marjou, F.E., and Louvard, D. (1999). Regulatory sequences of the mouse villin gene that efficiently drive transgenic expression in immature and differentiated epithelial cells of small and large intestines. J. Biol. Chem. *274*, 6476–6482.

Polakis, P. (2000). Wnt siganlling and cancer. Genes Dev. *14*, 1837–1851.

Potten, C.S., and Loeffler, M. (1990). Stem cells: attributes, cycles, spirals, pitfalls and uncertainties. Lessons for and from the crypt. Development *110*, 1001–1020.

Robinson, V., Smith, A., Flenniken, A.M., and Wilkinson, D.G. (1997). Roles of Eph receptors and ephrins in neural crest pathfinding. Cell Tissue Res. *290*, 265–274.

Schaller, M.D., and Parsons, J.T. (1995). pp125FAK-dependent tyrosine phosphorylation of paxillin creates a high-affinity binding site for Crk. Mol. Cell. Biol. *15*, 2635–2645.

Schmucker, D., and Zipursky, S.L. (2001). Signaling downstream of Eph receptors and ephrin ligands. Cell *105*, 701–704.

Shamah, S.M., Lin, M.Z., Goldberg, J.L., Estrach, S., Sahin, M., Hu, L., Bazalakova, M., Neve, R.L., Corfas, G., Debant, A., and Greenberg, M.E. (2001). EphA receptors regulate growth cone dynamics through the novel guanine nucleotide exchange factor Ephexin. Cell *105*, 233–244.

Stappenbeck, T.S., Wong, M.H., Saam, J.R., Mysorekar, I.U., and Gordon, J.I. (1998). Notes from some crypt watchers: regulation of renewal in the mouse intestinal epithelium. Curr. Opin. Cell Biol. *10*, 702–709.

van de Wetering, M., Sancho, E., Verweij, C., de Lau, W., Oving, I., Hurlstone, A., van der Horn, K., Batlle, E., Coudreuse, D., Haramis, A.-P., et al. (2002). The β-catenin/TCF4 complex imposes a crypt progenitor phenotype on colorectal cancer cells. Cell *111*, this issue, 241–250.

Wilkinson, D.G. (2001). Multiple roles of Eph receptors and ephrins in neural development. Nat. Rev. Neurosci. *2*, 155–164.

Wilkinson, D.G. (2000). Topographic mapping: organising by repulsion and competition? Curr. Biol. *10*, R447–R451.

Xu, Q., Alldus, G., Holder, N., and Wilkinson, D.G. (1995). Expression of truncated Sek-1 receptor tyrosine kinase disrupts the segmental restriction of gene expression in the *Xenopus* and zebrafish hindbrain. Development *121*, 4005–4016.

Xu, Q., Mellitzer, G., Robinson, V., and Wilkinson, D.G. (1999). In vivo cell sorting in complementary segmental domains mediated by Eph receptors and ephrins. Nature *399*, 267–271.